CLINICAL AND VACCINE IMMUNOLOGY, Sept. 2009, p. 1293–1301 Vol. 16, No. 9
1556-6811/09/$08.00+0 doi:10.1128/CVI.00074-09

Antiretroviral Therapy Restores Diversity in the T-Cell Receptor Vβ Repertoire of CD4 T-Cell Subpopulations among Human Immunodeficiency Virus Type 1-Infected Children and Adolescents▽

Li Yin,[1] Zhong Chen Kou,[1] Carina Rodriguez,[3] Wei Hou,[2] Maureen M. Goodenow,[1] and John W. Sleasman[4]*

Departments of Pathology, Immunology and Laboratory Medicine[1] and Department of Epidemiology and Health Policy Research,[2] Shands Cancer Center, University of Florida, College of Medicine, Gainesville, Florida, and Division of Infectious Diseases[3] and Division of Allergy, Immunology, and Rheumatology,[4] University of South Florida, College of Medicine, St. Petersburg, Florida

Received 19 February 2009/Returned for modification 8 April 2009/Accepted 2 July 2009

Human immunodeficiency virus (HIV) type 1 infection perturbs the T-cell receptor (TCR) Vβ repertoire. The TCR CDR3 length diversity of individual Vβ families was examined within CD45RA and CD45RO CD4 T cells to assess the impact of the virus on clonality throughout CD4 T-cell activation and differentiation. A cross-sectional and longitudinal cohort study of 13 HIV-infected and 8 age-matched healthy children and adolescents examined the Vβ CDR3 length profiles within CD4 T-cell subsets by the use of spectratyping. HIV-infected subjects demonstrated higher numbers of perturbations in CD4 CD45RA T cells (5.8 ± 4.9 Vβ families) than healthy individuals (1.6 ± 1.8 Vβ families) ($P = 0.04$). Surprisingly, CD4 CD45RO central memory T cells from infected subjects showed no increased perturbations compared to the perturbations for the same cells from healthy subjects (2.9 ± 3.1 and 1.1 ± 1.8 Vβ families, respectively; $P = 0.11$). CD4 CD45RA TCR perturbations were higher among infected subjects with >25% CD4 cells than healthy subjects (mean number of perturbed Vβ families, 6.6 ± 5.4; $P = 0.04$). No correlations between perturbations in CD4 subsets and pretherapy age or viral load were evident. In contrast to CD8 T cells, HIV induces TCR disruptions within CD45RA but not CD45RO CD4 T cells. Therapy-induced viral suppression resulted in increases in thymic output and the normalization of the diversity of TCR within CD45RA CD4 T cells after 2 months of treatment. Perturbations occur prior to CD4 T-cell attrition and normalize with effective antiretroviral therapy. The impact of HIV on the diversity of TCR within naïve, central memory, and effector memory CD4 T cells is distinctly different from that in CD8 T cells.

Human immunodeficiency virus type 1 (HIV-1) infection alters T-cell homeostasis by both impairing thymic output and inducing chronic T-cell activation. These disruptions are manifest by the increased level of expression of T-cell activation markers and decreased numbers of naïve T cells from the thymus (10, 12, 51). Oligoclonal T-cell expansion results in perturbations of the T-cell receptor (TCR) Vβ repertoire within both CD4 and CD8 T cells, with CD8 T cells being affected to a greater extent than CD4 T cells (7, 12, 16, 29, 50). Many of these abnormalities occur prior to CD4 T-cell attrition and are not fully reconstituted when viral replication is controlled by antiretroviral therapy (6, 17, 30). Multiple mechanisms have been postulated to contribute to this processes of aberrant T-cell activation and clonal expansion, including microbial translocation across the gastrointestinal tract as a result of virus-induced intestinal fibrosis (4, 5, 40) and the loss of immune regulation due to chronic HIV-induced antigenemia (8, 22).

CD4 and CD8 T cells are heterogeneous populations that differ functionally and in their expression of activation and differentiation markers, forming the basis of their classification as naïve, central memory (CM), or effector memory (EM) T cells (42). Isoforms of CD45 (CD45RA and CD45RO) are frequently used to subdivide CD4 and CD8 T cells into functional subsets (1, 13, 25, 44, 45). Oligoclonal expansions and deletions within T-cell subpopulations can be measured by analysis of the hypervariable CDR3 region of the TCR (37). CDR3 length variation reflects changes within the TCR Vβ repertoire during antigen-induced T-cell activation (24, 25, 34). Differences in CDR3 length diversity within the CD4 or the CD8 CD45RA or CD45RO subset enable assessments of disruptions of the TCR repertoire and the detection of oligoclonal expansion that would have been missed if the analysis were limited to unfractionated T cells (25, 26). While optimal control of viral replication by antiretroviral therapy (ART) corrects many T-cell abnormalities and slows the progression to AIDS, it is not clear if therapy completely restores the TCR repertoire or fully diminishes T-cell activation (7, 14, 27, 51). In the present study, we examined the relationship of TCR diversity, thymic output, and the expression of T-cell activation markers within the CD45RA and CD45RO subpopulations of CD4 and CD8 T cells before and after the initiation of ART to determine the extent to which the control of viral replication restores the TCR repertoire.

* Corresponding author. Mailing address: Division of Allergy, Immunology & Rheumatology, Department of Pediatrics, University of South Florida/All Children's Hospital, 801 Sixth Street South (Box 9350), St. Petersburg, FL 33701. Phone: (727) 767-4470. Fax: (727) 767-8542. E-mail: jsleasma@health.usf.edu.

▽ Published ahead of print on 15 July 2009.

MATERIALS AND METHODS

Subjects. Thirteen HIV-infected children and adolescents, including four patients evaluated before and after the initiation of combination ART consisting of

two nucleoside reverse transcriptase inhibitors and a protease inhibitor or a nonnucleoside reverse transcriptase inhibitor, provided blood samples for analysis in this cross-sectional and longitudinal study. The control subjects included eight age-matched healthy subjects who had no underlying medical condition, recent illness, or immunizations. Informed consent for the collection and analysis of blood samples was obtained from the institutional review boards of the University of Florida and the University of South Florida/All Children's Hospital.

The plasma HIV-1 RNA copy number was measured by an assay with the Amplicor (version 1.0) system (Roche Molecular Systems, Pleasanton, CA), which has a lower limit of detection of 400 copies/ml. T-cell subset analysis was performed by flow cytometry prior to and at 4-week intervals after the initiation of ART (46).

Isolation and purification of T-lymphocyte subsets. Peripheral blood mononuclear cells (PBMCs) were separated into T-cell subpopulations, as described previously (25, 44). Briefly, CD4 T lymphocytes were selected with magnetic multisort microbeads coated with anti-CD4 monoclonal antibodies (MAbs) and a magnetic cell-sorting high-gradient magnetic separation column. After CD4 depletion, CD8 T cells were selected with microbeads coated with an anti-CD8 MAb (Miltenyi Biotech, Auburn, CA). Purified CD4 or CD8 cells were separated into the CD45RA and CD45RO subpopulations by using microbeads coated with the appropriate MAb (mouse immunoglobulin G1, clone L48, for CD45RA and mouse immunoglobulin G2a for CD45RO; Miltenyi Biotech). The purity of each T-cell subpopulation was >95%, as determined by flow cytometry and molecular analysis, with <1% contamination with the reciprocal subpopulation being detected (43, 44).

Assessment of TRECs in PBMCs. The frequency of signal-jointing TCR receptor excision circles (TRECs) in PBMCs was quantified by real-time quantitative PCR with the primers and fluorogenic probe described previously (51). Data were expressed as the $\log_{10}$ number of TREC copies per 10^6 PBMCs by using the mean values for triplicate TRECs and duplicate ApoB TaqMan assays.

Flow cytometry analysis of CD4 T-cell subsets. PBMCs from the study subjects were incubated with the respective antibody combinations for 30 min in phosphate-buffered saline buffer containing 2% fetal calf serum and 0.1% sodium azide. The cells were then washed twice, fixed with 1% paraformaldehyde, and analyzed with a multiparametric LSR 2 flow cytometer (BD Biosciences, Franklin Lakes, NJ), as described previously (51). $CD4^+$ T-cell subsets were defined as follows: naïve CD4 T cells, $CD3^+$ $CD4^+$ $CD45RA^+$ $CD27^+$ $CD28^+$; EM CD4 T cells, $CD3^+$ $CD4^+$ $CD45RA^+$ $CD27^-$ $CD28^-$; and CM CD4 T cells, $CD3^+$ $CD4^+$ $CD45RO^+$ $CD27^-$ $CD28^-$ (32, 39, 51).

Measurement of CDR3 length variation. TCR CDR3 for each Vβ family was amplified by using 0.5 μl of 20 μl cDNA generated from mRNA extracted from the CD45RA or CD45RO subset of CD4 or CD8 T cells. Insufficient template mRNA resulted in an artificially distorted CDR3 length distribution (Fig. 1A), characterized as CDR3 lengths with warble baselines, low fluorescence intensities (FI; <400), and a missing length(s) (Fig. 1A, Vβ13) or the complete loss of CDR3 peaks (Fig. 1A, Vβ17). To ensure that a sufficient amount of template was used to amplify each Vβ family, template optimization was performed with cord blood cells and T cells purified from PBMCs of a healthy adult. The minimum amount of mRNA able to produce a Gaussian distribution of CDR3 lengths was defined by serial dilution of input template equivalent to 10.0 ng to 0.6 ng mRNA from 25.0×10^4 to 1.6×10^4 purified T cells from a cord blood sample (Fig. 1B). The minimal amount of template mRNA capable of producing a Gaussian distribution for Vβ2 was 1.3 ng (equivalent to 3.1×10^4 purified T cells), and two long CDR3 length peaks started to diminish at 0.6 ng. At an mRNA level of 1.3 ng, the CDR3 length repertoires of 18 Vβ families within CD45RA and CD45RO CD8 T-cell subsets were amplified from a healthy adult (Fig. 1C), and most families showed a Gaussian distribution. Families (the Vβ15 family within CD8 CD45RA T cells and the Vβ11, Vβ14, Vβ15, and Vβ18 families within CD8 CD45RO T cells) showing clonal expansion were true perturbations rather than template insufficiency because of a stable baseline and normal FIs. In this study, lymphocyte mRNA was isolated from 1×10^5 to 5×10^5 purified T lymphocytes (25, 26). First-strand cDNA was synthesized from 4 to 20 ng of mRNA, which was more than the minimum amount of template mRNA required (1.3 ng), by using 1 μg of random hexanucleotides (Promega, Madison, WI) and 5 μl of Supertranscriptase II (Gibco BRL, Grand Island, NY) in a 20-μl volume, and 0.5 μl of 20 μl cDNA was used to amplify each Vβ family. This range of input template mRNA was sufficient to consistently obtain a Gaussian distribution of CDR3 lengths for 21 Vβ families from the eight age-matched healthy controls in this study, unless there was a true perturbation. Figure 1D exemplifies the Gaussian distribution of CDR3 lengths of all 21 Vβ families within the CD45RA and CD45RO CD4 T-cell subsets from one 15-year-old healthy control in this study.

Analysis of the CDR3 size within the TCR β chain was performed by a two-step PCR through separate amplification reactions for each of 21 human Vβ families (25, 26). An initial denaturing step of 3 min at 95°C was followed by 35 cycles of 95°C for 1 min, 55°C for 1 min, 72°C for 1 min, with a final extension at 72°C for 7 min.

The second-round PCR used the first-round PCR products as the template and a pair of nested PCR primers. The forward primer (primer VβNS) was nested 3′ to the first-round Vβ-specific primer, and the reverse primer (primer CβNS) was located 88 bp away from the CDR3 region (25). The reverse primer (primer CβNS) contained a nontemplate sequence (GTTTCTT) and a blue fluorescent dye (6-carboxyfluorescein; Applied Biosystems, Foster City, CA) at the 5′ end.

The fluorescent PCR product and a size marker (red, ROX400; Applied Biosystems) were mixed with formamide, denatured at 94°C for 2 min, loaded on a 6% acrylamide sequencing gel (National Diagnostic, Atlanta, GA), and resolved on an ABI model 373 DNA sequencer (Applied Biosystems). The data were analyzed with ABI Prism GeneScan analysis software.

Quantitative analysis of CDR3 length profiles. The TCR CDR3 length distribution in each of the 21 Vβ families from the CD45RA and CD45RO CD4 and CD8 T-cell subsets in the group of eight healthy children who were age matched with the HIV-infected cohort was examined.

The calculated area under the curve for each CDR3 length (i) in a Vβ family profile (κ) was translated into a probability distribution, $P^{\kappa}_j(i) = A^{\kappa}_{j,i}/(\Sigma_i A^{\kappa}_{j,i})$, where the letter j represents each sample, by using the fraction of the area (A_i) under the Vβ family profile for each CDR3 length from the minimal to the maximal length in steps of 3 nucleotides. Generally, there were 10 possible amino acid lengths (i_1 to i_{10}) in each Vβ family. A control profile was established for each CDR3 length by calculating the average probability distribution, $P^{\kappa}_c(i) = \{\Sigma_j [P^{\kappa}_j(i)]\}/n_j$, where n represents the number of healthy subjects, of the corresponding Vβ profiles. The resulting control profiles, $P^{\kappa}_c(i)$, conform to a Gaussian distribution.

To define the extent of perturbations in CDR3 length, the distance (D) between the probability distributions of the samples and the average probability distributions for the healthy controls (c) was calculated as $D^{\kappa}_j(i) = P^{\kappa}_j(i) - P^{\kappa}_c(i)$. The sum of the absolute distance, $D^{\kappa}_j = 100\,[\Sigma_i\ D^{\kappa}_j(i)\ ]/2$, was calculated for each Vβ family. Overall, the TCR length yields the perturbations of the TCR profile in percent. The average perturbation among all Vβ families studied for each individual j was calculated as an average distance (AD), $\mathrm{AD}_j = (\Sigma^{\kappa} D^{\kappa}_j)/m^{\kappa}$, where m is the number of all Vβ families examined. In this study, the average distance for a control sample is presented as $\mathrm{AD}_c(j) = (\Sigma^{\kappa} D^{\kappa}_j)/m^{\kappa}$. On the basis of the approximate Z test, a perturbation within each Vβ family was defined as $\mathrm{AD}^{\kappa}_j > [\Sigma_j \mathrm{AD}_c(j)]/n_j + 3$ standard deviations (26).

Statistical analysis. Statistical analysis was performed with SAS (version 9.1) software (SAS Institute, Cary, NC). To accommodate the sample size and the nature of the pilot data, all variables were $\log_{10}$ transformed, and P values of <0.05 were considered significant. Comparison of the variables between the HIV-infected and the healthy individuals or within each group was performed by t test. The Pearson correlation coefficient was used to study the relationship of the number of perturbed Vβ families within the CD45RA and CD45RO CD4 T-cell subsets with the clinical variables. The paired t test was used to compare the number of perturbed Vβ families within the CD4 CD45RA and CD45RO T-cell subsets in HIV-infected subjects before and after therapy.

RESULTS

TCR CDR3 length profiles in CD4 T-cell subpopulations of healthy children. The TCR CDR3 length profiles within CD4 CD45RA and CD45RO T cells from eight healthy children (median age, 6.5 ± 6.0 years) were evaluated to establish the normal CDR3 diversity ranges. On the basis of the calculations for the healthy subjects, a perturbation in CD4 CD45RA T cells was defined as a D^{κ}_j value of >11.76% per Vβ family, that is, $[\Sigma_j\ \mathrm{AD}_c(j)]/n_j + 3$ standard deviations = 7.74% + (3 × 1.34%) = 11.76%, and similarly, a perturbation in CD4 CD45RO T cells was defined as a D^{κ}_j value of >19.87%.

Among the healthy children, the Vβ families within CD4 T cells displayed few perturbations (Fig. 2A). The mean number of perturbed Vβ families (NP) was 1.6 ± 1.8 in the CD45RA subset and 1.1 ± 1.8 in the CD45RO subset. No perturbations in either CD4 T-cell subset were detected in 11 of 21 (52%) Vβ

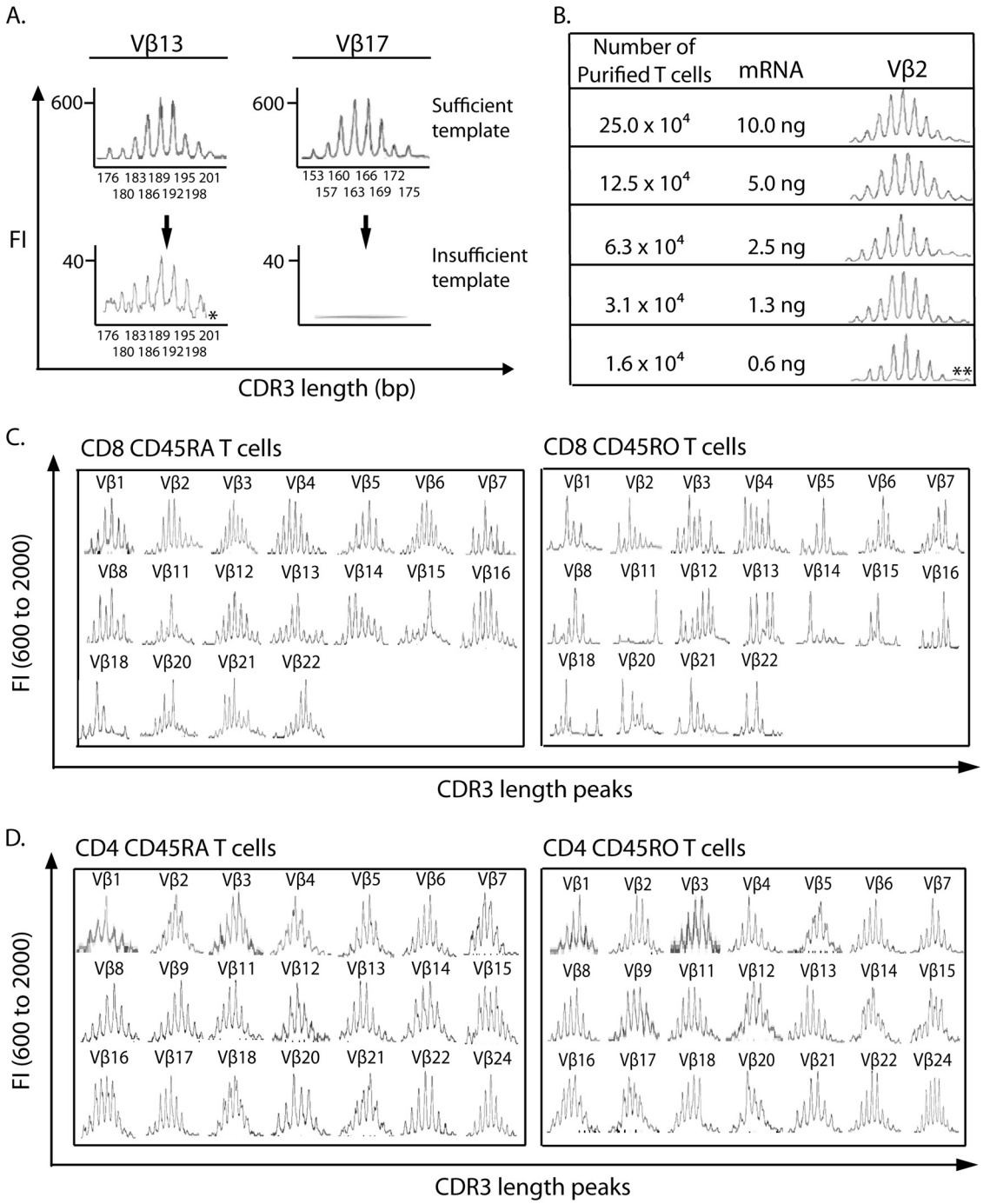

FIG. 1. Optimization of input template mRNA to avoid distortion of CDR3 length distribution resulting from template insufficiency. (A) CDR3 length distributions distorted by insufficient template were characterized as a warble baseline, low FI, and missing length peak of 201 bp in Vβ13 and a complete loss of length peaks in Vβ17. (B) Amplification of Vβ2 using serially diluted template mRNA at concentrations ranging from 10 ng (from 25.0×10^4 purified T cells) to 0.6 ng (from 1.6×10^4 purified T cells). The minimum amount of template mRNA able to generate a Gaussian distribution of CDR3 lengths was 1.3 ng. Two long CDR3 length peaks (**) diminished at the 0.6-ng level. (C) TCR CDR3 within CD45RA and CD45RO CD8 T cells from a healthy adult was amplified for 18 Vβ families by using 1.3 ng mRNA template. All Vβ families were amplified without a baseline oscillation and with the FI within the normal range, including Vβ families showing clonal expansion (Vβ15 within CD8 CD45RA T cells and Vβ11, Vβ14, Vβ15, and Vβ18 within CD8 CD45RO T cells). (D) Representative TCR CDR3 length distribution of all 21 Vβ families within CD45RA and CD45RO CD4 T cells from a 15-year-old healthy subject with the amount of template (4 to 20 ng mRNA) used for this study. The CDR3 lengths of all Vβ families showed Gaussian distributions.

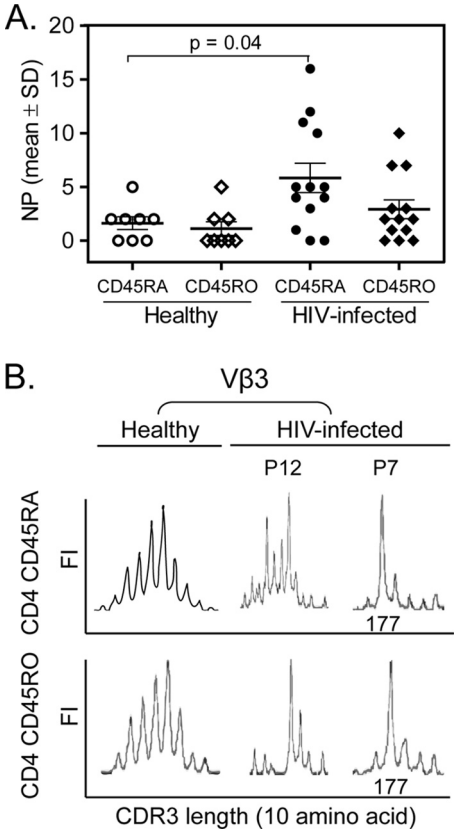

FIG. 2. TCR CDR3 Vβ perturbations within CD45RA and CD45RO CD4 T-cell subsets from healthy and therapy-naïve HIV-infected children and adolescents. (A) NPs within CD45RA and CD45RO CD4 T-cell subsets from healthy and HIV-infected therapy-naïve pediatric patients. The NP within CD4 CD45RA T cells was significantly greater for HIV-infected subjects than for the age-matched healthy controls ($P = 0.04$). There was no significant difference in the NPs in CD4 CD45RO T cells between HIV-infected and healthy subjects ($P = 0.11$). (B) TCR CDR3 Vβ3 perturbations within CD45RA and CD45RO CD4 T-cell subsets presented as either a single predominant peak, as shown for patient P7, or multiple peaks but statistically away from a Gaussian distribution for a healthy control, as demonstrated for patient P12.

families, including Vβ families 2, 3, 4, 6, 7, 8, 12, 13 18, 20, and 22. The difference between the NPs in CD4 CD45RA and CD45RO T cells was not significant ($P = 0.17$, t test).

TCR CDR3 length distributions in CD4 T-cell subpopulations from HIV-1-infected children before highly active ART. The TCR CDR3 length diversity in CD45RA and CD45RO CD4 T-cell subsets from 13 therapy-naïve HIV-infected children and adolescents was examined prior to the initiation of ART (Table 1). The mean age of these children was 9.8 ± 7.9 years, which was similar to the mean age of the corresponding healthy cohort ($P = 0.25$, t test). The mean CD4 T-cell counts pretherapy were in the normal range of 882 ± 833 cells/μl (31.5% ± 7.9%). Within the CD4 T cells, the absolute number and the percentage of the T-cell subsets were 666 ± 836 cells/μl and 66.8% ± 15.4%, respectively, for CD45RA T cells and 215 ± 73.4 cells/μl and 33% ± 15.3%, respectively, for CD45RO T cells. The absolute CD8 T-cell counts and percentages were 906 ± 446 cells/μl and 37.5% ± 11.9%, respectively. The mean $\log_{10}$ HIV-1 RNA load was 4.2 ± 1.1 copies/ml.

Compared to the healthy individuals, the HIV-infected children and adolescents demonstrated a significantly higher number of perturbations within Vβ families of CD4 CD45RA T cells (mean NP, 5.8 ± 4.9; $P = 0.04$, t test) (Fig. 2A). In contrast, there was no significant difference in NPs for CD45RO CD4 T cells between the HIV-infected cohort (mean NP, 2.9 ± 3.1) and the healthy cohort ($P = 0.11$, t test) (Fig. 2A). The CDR3 length perturbations differed within the CD4 CD45RA and CD45RO T-cell subsets. With TCR Vβ3 as an example (Fig. 2B), the Vβ perturbation fell into two types. One showed a single predominant length peak that represented more than 40% of the total area under the curve, as presented by patient P7, and the other showed multiple length peaks that differed statistically from a Gaussian distribution, as demonstrated by patient P12. Each formed a distinct contrast to the Gaussian distribution of TCR CDR3 lengths in the healthy controls.

Among the individuals in the infected population with relatively normal CD4 T-cell counts, the pretherapy NP within CD4 CD45RA or CD45RO T cells showed no correlation with age, the length of infection, the viral load, the percentage of CD4 or CD8 cells, or the proportion of CD45RA or CD45RO CD4 T cells. Perturbations within the CD4 CD45RA T-cell subsets in 10 HIV-infected subjects with CD4 T-cell counts of greater than 25% were compared to the perturbations within the CD4 CD45RA T-cell subsets in healthy subjects to determine if the TCR repertoire was disrupted prior to CD4 T-cell attrition. Among these subjects, CD4 CD45RA had a significantly higher NP in the infected group than in the healthy group (NPs, 6.6 ± 5.4 and 1.6 ± 1.8, respectively; $P = 0.04$, t test).

Comparison of TCR CDR3 length distribution in CD4 and CD8 T-cell naïve and memory subpopulations in HIV-infected children before highly active ART. In six infected patients (patients P3, P4, P5, P6, P7, and P11), the CD4 and CD8 subpopulations were obtained at the same time point to examine the TCR CDR3 length diversity before the initiation of ART (Fig. 3). The mean NP within CD4 CD45RA T cells for these six patients was 7.5 ± 5.9, similar to the mean NP in CD8 CD45RA T cells (9.5 ± 4.8) ($P = 0.41$, t test) (Fig. 3A, upper panel). In contrast, the mean NP for CD4 CD45RO T cells was 2.5 ± 2.4, which was significantly lower than the NP for CD8 CD45RO of 14.0 ± 5.0 ($P = 0.003$, t test) (Fig. 3A, lower panel). Figure 3B shows the TCR CDR3 distributions within the CD4 and CD8 T-cell subpopulations in Vβ9, Vβ15, Vβ18, and Vβ22 in patient P3. All four Vβ families were perturbed in CD45RA CD4 and CD8 T cells and in CD45RO CD8 T cells but not in CD45RO CD4 T cells.

Impact of ART on T-cell activation markers and TCR CDR3 length diversity in CD4 CD45RA and CD45RO subpopulations. A longitudinal analysis of the changes in CDR3 length diversity within CD4 CD45RA and CD45RO T cells over the first 24 weeks of combination ART was performed for four children (patients P3, P4, P5, and P7) who fully suppressed viral replication by 2 months after the start of treatment (Fig. 4A). The mean NP for CD4 CD45RA T cells for the group prior to treatment was 10.5 ± 4.5, which declined to 3.5 ± 2.9 following 2 to 6 months of therapy ($P = 0.10$, paired t test)

TABLE 1. Baseline demographic, viral, and immune characteristics of study group

PID[a]	Age (yr)	Gender[b]	Ethnicity	HIV-1 RNA load (log_{10} no. of copies/ml)	CD4		CD8		CD4			
									CD45RA		CD45RO	
					%[c]	No. of cells/ml	%[c]	No. of cells/ml	%[d]	No. of cells/ml	%[d]	No. of cells/ml
P1	0.2	F	Black	5.8	43	3,491	23	1,867	95	3,316	5	175
P2	0.3	F	Black	6.8	19	371	17	332	82	304	17	63
P3	4.2	F	Black	3.2	34	821	28	676	76	624	25	205
P4	4.3	F	Caucasian	4.1	45	1,332	32	947	81	1,079	19	253
P5	5.0	M	Black	4.3	22	673	55	1,683	47	316	53	357
P6	6.2	M	Hispanic	3.7	31	986	30	955	71	700	28	276
P7	6.9	F	Black	3.5	31	379	47	575	68	258	38	144
P8	7.5	M	Caucasian	4.9	35	886	43	1,088	75	665	25	222
P9	11.1	F	Black	4.1	31	568	50	917	63	358	35	199
P10	19.4	F	Black	4.8	37	654	39	689	57	372	43	281
P11	19.9	F	Black	2.9	33	446	40	541	63	280	36	161
P12	20.1	M	Caucasian	3.5	27	469	30	521	47	220	55	258
P13	22.3	M	Black	3.6	21	389	53	981	44	171	53	206

[a] PID, patient identification. For patients P10, P11, and P12, the source of infection was sexual transmission; for patient P13 the source of infection was blood transmission; for all other patients, the source of infection was maternal transmission.
[b] F, female; M, male.
[c] Percentage of lymphocytes.
[d] Percentage of $CD4^+$ T cells.

(Fig. 4A, left panel). The mean pretherapy NP for CD4 CD45RO T cells was 3.3 ± 2.6, which decreased further to 0.3 ± 0.5 within 2 to 6 months of treatment ($P = 0.06$, paired t test) (Fig. 4A, right panel). The NP within either CD4 T-cell subset after 1 year of therapy was similar to the NP at 2 months posttreatment in patients P3 and P7. Figure 4B exemplifies the restoration of a Gaussian distribution of the CDR3 length repertoire after 2 months and 1 year of optimal viral suppression. In patient P7, there was a predominant CDR3 length peak in both Vβ3 and Vβ16 within the CD45RA and CD45RO CD4 T-cell subsets. These predominant peaks were identical in both subsets, on the basis of CDR3 lengths of 177 and 159 bp, respectively. By 2 months after the start of treatment, this oligoclonal expansion had resolved. The posttherapy NP within both CD4 T-cell subsets among the four HIV-infected subjects decreased to the levels found in healthy children ($P = 0.31$ for NP within CD4 CD45RA T cells and $P = 0.42$ for NP within CD4 CD45RO T cells).

To determine if changes in the TCR Vβ repertoire within CD4 CD45RA and CD45RO T cells correlated with changes in the TREC level and phenotypic shifts within CD4 T-cell subsets, the log_{10} number of TREC copies/10^6 PBMCs was evaluated by real-time quantitative PCR; and the absolute numbers and percentages of CD4 naïve, EM, and CM T cells in three of the suppressed subjects whose TCR Vβ repertoire was evaluated longitudinally were assessed by multiparameter flow cytometry analysis. The TREC levels increased in patients P3 and P7 and remained unchanged in patient P5, whose TREC level was normal for age before therapy (Fig. 4C, panel a). In all three subjects, the absolute number of naïve CD4 T cells increased and the number of EM CD4 T cells was unchanged (Fig. 4C, panels b and c, respectively). However, despite the decreased NP within CD4 CD45RA T cells, there was no evident shift in the percentage of naïve or EM CD45RA subsets. The absolute number of CD45RO CM T cells increased in all three subjects (Fig. 4C, panel d), but the percentage remained similar and was unrelated to the changes in NP within total CD4 CD45RO T cells.

DISCUSSION

There have been few assessments of the impact of HIV replication on the TCR repertoire within both CD4 and CD8 T subsets. The findings of this study, along with those of our previous studies, provide new insight into the extent that viral replication disrupts T-cell differentiation by measuring TCR diversity within the distinct naïve, CM, and EM T-cell subsets in HIV-infected individuals (25, 26, 51). Examination of the TCR repertoire within T cells at different stages of activation and differentiation enables sensitive assessment of how viral replication skews T-cell development by inducing oligoclonal T-cell expansion within EM and CM T cells. The study provides greater insight into perturbations within the TCR repertoire than analysis of unfractionated CD4 or CD8 T cells (25).

Overall, the TCR Vβ repertoire is less perturbed in CD4 T cells than in CD8 T cells in healthy children and adolescents (16, 18, 33, 47). Our results show that in healthy children, CD8 T-cell perturbations are primarily the result of oligoclonal expansions within CD8 CD45RO T cells (26). In contrast, there are surprisingly few perturbations within circulating CD4 CD45RO T cells. The extent of perturbations in CD8 T-cell subsets is likely due to cytokine-driven memory CD8 T cells that are independent of continued antigen stimulation, which allows cells to persist in the blood over time (49). In contrast, preserved Gaussian distributions within CD4 CD45RO T cells could be the result of fewer clonally expanded HIV-specific CD4 T cells or antigen-induced homing of clonally expanded CD4 T cells to inflammatory sites or lymphoid tissues (6, 15, 23, 28).

HIV infection affects CD4 and CD8 T-cell subsets differently. In general, the degree of HIV-induced oligoclonal expansion in CD4 T cells is less than that in CD8 T cells (2, 16,

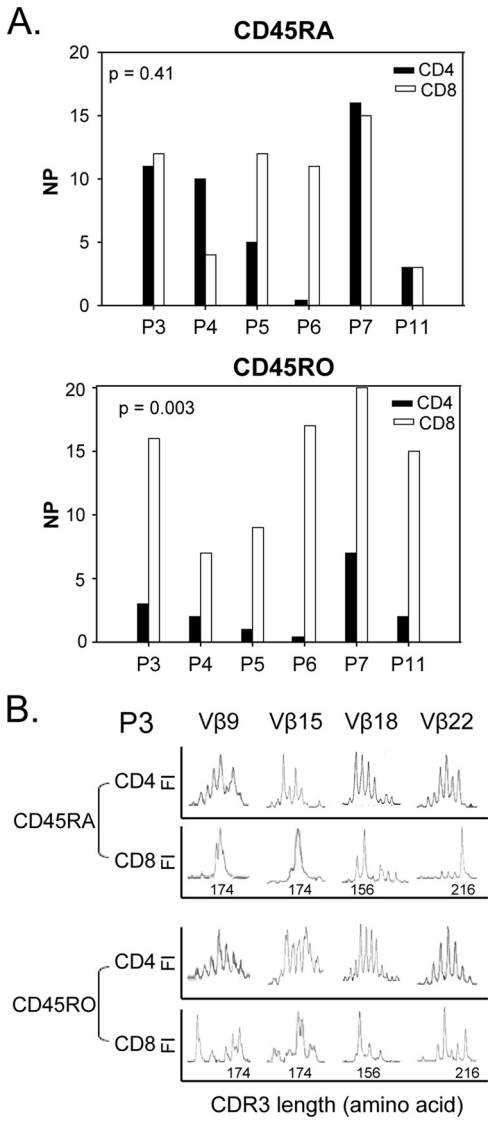

FIG. 3. Comparison of TCR CDR3 Vβ perturbations within CD4 and CD8 T-cell subpopulations among six therapy-naïve HIV-infected subjects. (A) NP within CD45RA and CD45RO subsets of CD4 and CD8 T cells in six HIV-infected subjects prior to therapy. The NP within CD4 CD45RA T cells was similar to that within CD8 CD45RA T cells ($P = 0.41$). The NP within CD8 CD45RO T cells was significantly higher than that within CD4 CD45RO T cells ($P = 0.003$). (B) TCR CDR3 length distribution in Vβ9, Vβ15, Vβ18, and Vβ22 in patient P3 was perturbed in CD45RA CD4 and CD8 T cells and CD45RO CD8 T cells but not in CD45RO CD4 T cells.

36, 38). One potential explanation is that viremia leads to a large proportion of activated HIV-specific cytotoxic T lymphocytes directed toward multiple antigenic epitopes (31, 35). The magnitude of HIV-specific cytotoxic T-cell responses does not predict the effectiveness of control of viral replication (10, 21). Multiple perturbations within the CD8 T-cell repertoire are associated with higher viral loads and lower CD4 T-cell counts (26) and could arise from viral immune escape as new antigenic epitopes emerge, resulting in less effective CD8 T-cell responses.

In the current study, no correlation between the viral burden or CD4 T-cell attrition and TCR perturbations within CD4 T-cell subsets was found. However, the cohort selected for study had relatively normal total CD4 T-cell counts (range, 432 to 911 cells/μl), and in general, the individuals in that cohort were asymptomatic. We and others have shown that many HIV-infected children and adolescents have intact thymic output and normal proportions of naïve T cells, as measured by the levels of TRECs and expression naïve T-cell surface markers (20, 33, 51). A novel finding in this study is the elevated level of perturbations within the CD4 and CD8 CD45RA subsets prior to the CD4 T-cell decline. The absence of perturbations within CD4 CD45RO T cells was particularly striking, particularly as this is the predominant subset that harbors HIV-1 in vivo (41, 43). Since HIV-specific memory CD4 T cells are preferentially infected, it would predict perturbations within this subset due to virus-induced expansion and apoptosis (11). It is likely that the small proportion of infected blood CD4 T cells results in a minimal impact on TCR diversity (2, 3, 6, 36). Overall, comparison of the perturbations within the CD45RA and CD45RO subpopulations emphasizes the differences in cellular dynamics between CD4 and CD8 T cells. CD8 CD45RA phenotypes within HIV-infected individuals display downregulated CCR7, CD27, and CD107 and increased levels of expression of activation markers, such as CD38, HLA-DR, and CD11a (1, 7, 19, 48, 51). Increased perturbations within CD8 CD45RA T cells correlate with CD4 T-cell suppression and a higher viral burden. This correlation is not evident when the TCR Vβ repertoire in CD4 CD45RA or CD45RO T cells is examined.

The viral suppression caused by ART results in the rapid reestablishment of a Gaussian distribution of CDR3 lengths in both the CD45RA and CD45RO CD4 T-cell subsets. The normalization is likely due to increases in thymic output, as demonstrated by increases in the levels of TRECs and CD4 T cells bearing a naïve phenotype (Fig. 4C, panels a and b), and represents a fundamental difference in T-cell immune reconstitution in infected young individuals (9, 16, 26, 51). The rapid reestablishment of CDR3 length diversity within CD4 CD45RA T cells in children and adolescents treated with combination ART is distinctly different from the kinetics of change in TCR diversity in treated adults (9, 16). The therapy-induced normalization of TCR diversity in both T-cell populations contributes to improved T-cell function (9, 16, 26, 38), reflecting the increased capacity of thymic output in children and adolescents. However, in the limited number of children and adolescents evaluated before and after ART, the absolute numbers of naïve and central memory T cells increased, yet the numbers of effector memory CD4 T cells were unchanged. While these results are consistent with those of previous studies of the cellular dynamics of the T-cell immune reconstitution in children, further studies are needed to examine the relationship of viral replication and virus-induced T-cell activation on EM CD4 T cells (46) In particular, the therapy-induced changes in TCR diversity in EM T cells following therapy need to be examined. We speculate that the therapy-induced normalization of TCR diversity in CD45RA T cells is most likely related to increases in naïve T cells from the thymus. In conclusion, this study is one of the first comprehensive evaluations of TCR diversity within CD4 and CD8 T cells along their differentiation pathways. It included children infected perina-

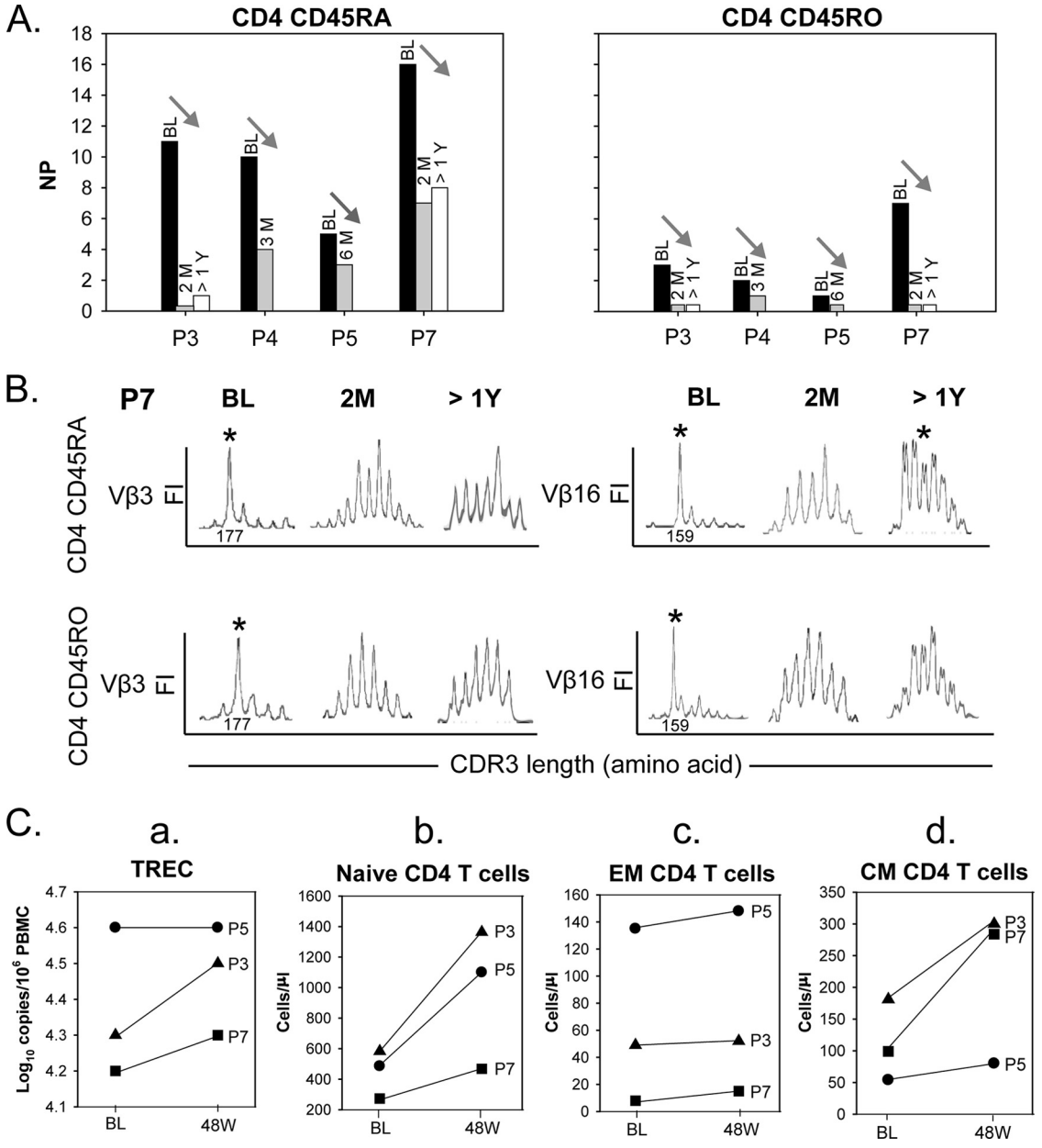

FIG. 4. Changes in TCR CDR3 Vβ profiles within CD45RA and CD45RO CD4 T cells and changes in TREC levels and the numbers of CD4 T-cell subpopulations after combination antiretroviral therapy. (A) Decrease in NPs within both CD45RA and CD45RO CD4 T cells from the baseline (BL), 2 to 6 months (M), and over 1 year (>1Y) posttherapy in patients P3, P4, P5, and P7. (B) Restoration of a Gaussian distribution of the TCR CDR3 length repertoire in Vβ3 and Vβ16 within CD45RA and CD45RO CD4 T-cell subsets from patients P7 at 2 months (2M) and 1 year (>1Y) after therapy. *, baseline oligoclonal expansions of 177- and 159-bp lengths within CD45RA and CD45RO T cells. (C) Change in $\log_{10}$ number of TREC copies/10^6 PBMCs (a) and changes in the number of naïve (b), EM (c), and CM (d) CD4 T cells (number of cells/μl) in three HIV-infected individuals (▲, patient P3; ●, patient P5; ■, patient P7) 48 weeks after therapy.

tally as well as adolescents infected through sexual transmission. The results reveal the precise points in T-cell development that HIV disrupts the TCR repertoire and shows how quickly the control of viral replication results in its normalization.

ACKNOWLEDGMENTS

This research was supported by PHS R01 awards HD032259, AI065265, and AI047723; the Pediatric Clinical Research Center of All Children's Hospital and the University of South Florida, Maternal Child Health Bureau (grant R60 MC 00003-01), U. S. Department of Health and Human Services, Resources and Services Administration; the University of Florida Center for Research for Pediatric Immune Deficiency; and the Stephany W. Holloway University Chair for AIDS Research (to M.M.G.).

REFERENCES

1. **Appay, V., and S. L. Rowland-Jones.** 2004. Lessons from the study of T-cell differentiation in persistent human virus infection. Semin. Immunol. **16:**205–212.
2. **Betts, M. R., D. R. Ambrozak, D. C. Douek, S. Bonhoeffer, J. M. Brenchley, J. P. Casazza, R. A. Koup, and L. J. Picker.** 2001. Analysis of total human

immunodeficiency virus (HIV)-specific $CD4^+$ and $CD8^+$ T-cell responses: relationship to viral load in untreated HIV infection. J. Virol. **75:**11983–11991.

3. **Brenchley, J. M., B. J. Hill, D. R. Ambrozak, D. A. Price, F. J. Guenaga, J. P. Casazza, J. Kuruppu, J. Yazdani, S. A. Migueles, M. Connors, M. Roederer, D. C. Douek, and R. A. Koup.** 2004. T-cell subsets that harbor human immunodeficiency virus (HIV) in vivo: implications for HIV pathogenesis. J. Virol. **78:**1160–1168.
4. **Brenchley, J. M., D. A. Price, and D. C. Douek.** 2006. HIV disease: fallout from a mucosal catastrophe? Nat. Immunol. **7:**235–239.
5. **Brenchley, J. M., D. A. Price, T. W. Schacker, T. E. Asher, G. Silvestri, S. Rao, Z. Kazzaz, E. Bornstein, O. Lambotte, D. Altmann, B. R. Blazar, B. Rodriguez, L. Teixeira-Johnson, A. Landay, J. N. Martin, F. M. Hecht, L. J. Picker, M. M. Lederman, S. G. Deeks, and D. C. Douek.** 2006. Microbial translocation is a cause of systemic immune activation in chronic HIV infection. Nat. Med. **12:**1365–1371.
6. **Brenchley, J. M., T. W. Schacker, L. E. Ruff, D. A. Price, J. H. Taylor, G. J. Beilman, P. L. Nguyen, A. Khoruts, M. Larson, A. T. Haase, and D. C. Douek.** 2004. $CD4^+$ T cell depletion during all stages of HIV disease occurs predominantly in the gastrointestinal tract. J. Exp. Med. **200:**749–759.
7. **Champagne, P., G. S. Ogg, A. S. King, C. Knabenhans, K. Ellefsen, M. Nobile, V. Appay, G. P. Rizzardi, S. Fleury, M. Lipp, R. Forster, S. Rowland-Jones, R. P. Sekaly, A. J. McMichael, and G. Pantaleo.** 2001. Skewed maturation of memory HIV-specific CD8 T lymphocytes. Nature **410:**106–111.
8. **Chinen, J., F. Finkelman, and W. T. Shearer.** 2006. Advances in basic and clinical immunology. J. Allergy Clin. Immunol. **118:**489–495.
9. **Connors, M., J. A. Kovacs, S. Krevat, J. C. Gea-Banacloche, M. C. Sneller, M. Flanigan, J. A. Metcalf, R. E. Walker, J. Falloon, M. Baseler, I. Feuerstein, H. Masur, and H. C. Lane.** 1997. HIV infection induces changes in $CD4^+$ T-cell phenotype and depletions within the $CD4^+$ T-cell repertoire that are not immediately restored by antiviral or immune-based therapies. Nat. Med. **3:**533–540.
10. **Dong, T., G. Stewart-Jones, N. Chen, P. Easterbrook, X. Xu, L. Papagno, V. Appay, M. Weekes, C. Conlon, C. Spina, S. Little, G. Screaton, A. van der Merwe, D. D. Richman, A. J. McMichael, E. Y. Jones, and S. L. Rowland-Jones.** 2004. HIV-specific cytotoxic T cells from long-term survivors select a unique T cell receptor. J. Exp. Med. **200:**1547–1557.
11. **Douek, D. C., J. M. Brenchley, M. R. Betts, D. R. Ambrozak, B. J. Hill, Y. Okamoto, J. P. Casazza, J. Kuruppu, K. Kunstman, S. Wolinsky, Z. Grossman, M. Dybul, A. Oxenius, D. A. Price, M. Connors, and R. A. Koup.** 2002. HIV preferentially infects HIV-specific $CD4^+$ T cells. Nature **417:**95–98.
12. **Douek, D. C., R. D. McFarland, P. H. Keiser, E. A. Gage, J. M. Massey, B. F. Haynes, M. A. Polis, A. T. Haase, M. B. Feinberg, J. L. Sullivan, B. D. Jamieson, J. A. Zack, L. J. Picker, and R. A. Koup.** 1998. Changes in thymic function with age and during the treatment of HIV infection. Nature **396:**690–695.
13. **Faint, J. M., N. E. Annels, S. J. Curnow, P. Shields, D. Pilling, A. D. Hislop, L. Wu, A. N. Akbar, C. D. Buckley, P. A. Moss, D. H. Adams, A. B. Rickinson, and M. Salmon.** 2001. Memory T cells constitute a subset of the human $CD8^+CD45RA^+$ pool with distinct phenotypic and migratory characteristics. J. Immunol. **167:**212–220.
14. **Ghaffari, G., D. J. Passalacqua, J. L. Caicedo, M. M. Goodenow, and J. W. Sleasman.** 2004. Two-year clinical and immune outcomes in human immunodeficiency virus-infected children who reconstitute CD4 T cells without control of viral replication after combination antiretroviral therapy. Pediatrics **114:**e604–e611.
15. **Goodnow, C. C., and J. G. Cyster.** 1997. Lymphocyte homing: the scent of a follicle. Curr. Biol. **7:**R219–R222.
16. **Gorochov, G., A. U. Neumann, A. Kereveur, C. Parizot, T. Li, C. Katlama, M. Karmochkine, G. Raguin, B. Autran, and P. Debre.** 1998. Perturbation of $CD4^+$ and $CD8^+$ T-cell repertoires during progression to AIDS and regulation of the $CD4^+$ repertoire during antiviral therapy. Nat. Med. **4:**215–221.
17. **Guadalupe, M., E. Reay, S. Sankaran, T. Prindiville, J. Flamm, A. McNeil, and S. Dandekar.** 2003. Severe $CD4^+$ T-cell depletion in gut lymphoid tissue during primary human immunodeficiency virus type 1 infection and substantial delay in restoration following highly active antiretroviral therapy. J. Virol. **77:**11708–11717.
18. **Halapi, E., M. Jeddi-Tehrani, A. Blucher, R. Andersson, P. Rossi, H. Wigzell, and J. Grunewald.** 1999. Diverse T-cell receptor CDR3 length patterns in human $CD4^+$ and $CD8^+$ T lymphocytes from newborns and adults. Scand. J. Immunol. **49:**149–154.
19. **Hamann, D., P. A. Baars, M. H. Rep., B. Hooibrink, S. R. Kerkhof-Garde, M. R. Klein, and R. A. van Lier.** 1997. Phenotypic and functional separation of memory and effector human $CD8^+$ T cells. J. Exp. Med. **186:**1407–1418.
20. **Holland, C. A., J. H. Ellenberg, C. M. Wilson, S. D. Douglas, D. C. Futterman, L. A. Kingsley, A. B. Moscicki, et al.** 2000. Relationship of $CD4^+$ T cell counts and HIV type 1 viral loads in untreated, infected adolescents. AIDS Res. Hum. Retrovir. **16:**959–963.
21. **Kalams, S. A., R. P. Johnson, A. K. Trocha, M. J. Dynan, H. S. Ngo, R. T. D'Aquila, J. T. Kurnick, and B. D. Walker.** 1994. Longitudinal analysis of T cell receptor (TCR) gene usage by human immunodeficiency virus 1 envelope-specific cytotoxic T lymphocyte clones reveals a limited TCR repertoire. J. Exp. Med. **179:**1261–1271.
22. **Kinter, A. L., M. Hennessey, A. Bell, S. Kern, Y. Lin, M. Daucher, M. Planta, M. McGlaughlin, R. Jackson, S. F. Ziegler, and A. S. Fauci.** 2004. $CD25^+CD4^+$ regulatory T cells from the peripheral blood of asymptomatic HIV-infected individuals regulate $CD4^+$ and $CD8^+$ HIV-specific T cell immune responses in vitro and are associated with favorable clinical markers of disease status. J. Exp. Med. **200:**331–343.
23. **Kirschner, D., G. F. Webb, and M. Cloyd.** 2000. Model of HIV-1 disease progression based on virus-induced lymph node homing and homing-induced apoptosis of $CD4^+$ lymphocytes. J. Acquir. Immune Defic. Syndr. **24:**352–362.
24. **Kostense, S., F. M. Raaphorst, J. Joling, D. W. Notermans, J. M. Prins, S. A. Danner, P. Reiss, J. M. Lange, J. M. Teale, and F. Miedema.** 2001. T cell expansions in lymph nodes and peripheral blood in HIV-1-infected individuals: effect of antiretroviral therapy. AIDS **15:**1097–1107.
25. **Kou, Z. C., J. S. Puhr, M. Rojas, W. T. McCormack, M. M. Goodenow, and J. W. Sleasman.** 2000. T-cell receptor Vβ repertoire CDR3 length diversity differs within CD45RA and CD45RO T-cell subsets in healthy and human immunodeficiency virus-infected children. Clin. Diagn. Lab. Immunol. **7:**953–959.
26. **Kou, Z. C., J. S. Puhr, S. S. Wu, M. M. Goodenow, and J. W. Sleasman.** 2003. Combination antiretroviral therapy results in a rapid increase in T cell receptor variable region beta repertoire diversity within CD45RA CD8 T cells in human immunodeficiency virus-infected children. J. Infect. Dis. **187:**385–397.
27. **Koup, R. A., J. T. Safrit, Y. Cao, C. A. Andrews, G. McLeod, W. Borkowsky, C. Farthing, and D. D. Ho.** 1994. Temporal association of cellular immune responses with the initial control of viremia in primary human immunodeficiency virus type 1 syndrome. J. Virol. **68:**4650–4655.
28. **Mackay, C. R.** 2000. Follicular homing T helper (Th) cells and the Th1/Th2 paradigm. J. Exp. Med. **192:**F31–F34.
29. **McCune, J. M.** 2001. The dynamics of $CD4^+$ T-cell depletion in HIV disease. Nature **410:**974–979.
30. **McMichael, A. J., and S. L. Rowland-Jones.** 2001. Cellular immune responses to HIV. Nature **410:**980–987.
31. **Ogg, G. S., X. Jin, S. Bonhoeffer, P. R. Dunbar, M. A. Nowak, S. Monard, J. P. Segal, Y. Cao, S. L. Rowland-Jones, V. Cerundolo, A. Hurley, M. Markowitz, D. D. Ho, D. F. Nixon, and A. J. McMichael.** 1998. Quantitation of HIV-1-specific cytotoxic T lymphocytes and plasma load of viral RNA. Science **279:**2103–2106.
32. **Oswald-Richter, K., S. M. Grill, M. Leelawong, M. Tseng, S. A. Kalams, T. Hulgan, D. W. Haas, and D. Unutmaz.** 2007. Identification of a CCR5-expressing T cell subset that is resistant to R5-tropic HIV infection. PLoS Pathog. **3:**e58.
33. **Pahwa, S., V. Chitnis, R. M. Mitchell, S. Fernandez, A. Chandrasekharan, C. M. Wilson, and S. D. Douglas.** 2003. $CD4^+$ and $CD8^+$ T cell receptor repertoire perturbations with normal levels of T cell receptor excision circles in HIV-infected, therapy-naive adolescents. AIDS Res. Hum. Retrovir. **19:**487–495.
34. **Pannetier, C., J. Even, and P. Kourilsky.** 1995. T-cell repertoire diversity and clonal expansions in normal and clinical samples. Immunol. Today **16:**176–181.
35. **Pantaleo, G., J. F. Demarest, H. Soudeyns, C. Graziosi, F. Denis, J. W. Adelsberger, P. Borrow, M. S. Saag, G. M. Shaw, and R. P. Sekaly.** 1994. Major expansion of $CD8^+$ T cells with a predominant V beta usage during the primary immune response to HIV. Nature **370:**463–467.
36. **Pitcher, C. J., C. Quittner, D. M. Peterson, M. Connors, R. A. Koup, V. C. Maino, and L. J. Picker.** 1999. HIV-1-specific $CD4^+$ T cells are detectable in most individuals with active HIV-1 infection, but decline with prolonged viral suppression. Nat. Med. **5:**518–525.
37. **Raaphorst, F. M., E. L. Kaijzel, M. J. van Tol, J. M. Vossen, and P. J. van den Elsen.** 1994. Non-random employment of V beta 6 and J beta gene elements and conserved amino acid usage profiles in CDR3 regions of human fetal and adult TCR beta chain rearrangements. Int. Immunol. **6:**1–9.
38. **Rosenberg, E. S., J. M. Billingsley, A. M. Caliendo, S. L. Boswell, P. E. Sax, S. A. Kalams, and B. D. Walker.** 1997. Vigorous HIV-1-specific $CD4^+$ T cell responses associated with control of viremia. Science **278:**1447–1450.
39. **Sallusto, F., J. Geginat, and A. Lanzavecchia.** 2004. Central memory and effector memory T cell subsets: function, generation, and maintenance. Annu. Rev. Immunol. **22:**745–763.
40. **Schacker, T. W., P. L. Nguyen, G. J. Beilman, S. Wolinsky, M. Larson, C. Reilly, and A. T. Haase.** 2002. Collagen deposition in HIV-1 infected lymphatic tissues and T cell homeostasis. J. Clin. Investig. **110:**1133–1139.
41. **Schnittman, S. M., S. M. Denning, J. J. Greenhouse, J. S. Justement, M. Baseler, J. Kurtzberg, B. F. Haynes, and A. S. Fauci.** 1990. Evidence for susceptibility of intrathymic T-cell precursors and their progeny carrying T-cell antigen receptor phenotypes TCR alpha beta + and TCR gamma delta + to human immunodeficiency virus infection: a mechanism for $CD4^+$ (T4) lymphocyte depletion. Proc. Natl. Acad. Sci. USA **87:**7727–7731.
42. **Seder, R. A., and R. Ahmed.** 2003. Similarities and differences in $CD4^+$ and $CD8^+$ effector and memory T cell generation. Nat. Immunol. **4:**835–842.

43. **Sleasman, J. W., L. F. Aleixo, A. Morton, S. Skoda-Smith, and M. M. Goodenow.** 1996. $CD4^+$ memory T cells are the predominant population of HIV-1-infected lymphocytes in neonates and children. AIDS **10:**1477–1484.
44. **Sleasman, J. W., B. H. Leon, L. F. Aleixo, M. Rojas, and M. M. Goodenow.** 1997. Immunomagnetic selection of purified monocyte and lymphocyte populations from peripheral blood mononuclear cells following cryopreservation. Clin. Diagn. Lab. Immunol. **4:**653–658.
45. **Sleasman, J. W., C. Morimoto, S. F. Schlossman, and T. F. Tedder.** 1990. The role of functionally distinct helper T lymphocyte subpopulations in the induction of human B cell differentiation. Eur. J. Immunol. **20:**1357–1366.
46. **Sleasman, J. W., R. P. Nelson, M. M. Goodenow, D. Wilfret, A. Hutson, M. Baseler, J. Zuckerman, P. A. Pizzo, and B. U. Mueller.** 1999. Immunoreconstitution after ritonavir therapy in children with human immunodeficiency virus infection involves multiple lymphocyte lineages. J. Pediatr. **134:**597–606.
47. **Soudeyns, H., P. Champagne, C. L. Holloway, G. U. Silvestri, N. Ringuette, J. Samson, N. Lapointe, and R. P. Sekaly.** 2000. Transient T cell receptor beta-chain variable region-specific expansions of $CD4^+$ and $CD8^+$ T cells during the early phase of pediatric human immunodeficiency virus infection: characterization of expanded cell populations by T cell receptor phenotyping. J. Infect. Dis. **181:**107–120.
48. **Weekes, M. P., A. J. Carmichael, M. R. Wills, K. Mynard, and J. G. Sissons.** 1999. Human $CD28^-CD8^+$ T cells contain greatly expanded functional virus-specific memory CTL clones. J. Immunol. **162:**7569–7577.
49. **Weninger, W., M. A. Crowley, N. Manjunath, and U. H. von Andrian.** 2001. Migratory properties of naive, effector, and memory $CD8^+$ T cells. J. Exp. Med. **194:**953–966.
50. **Wilson, J. D., G. S. Ogg, R. L. Allen, P. J. Goulder, A. Kelleher, A. K. Sewell, C. A. O'Callaghan, S. L. Rowland-Jones, M. F. Callan, and A. J. McMichael.** 1998. Oligoclonal expansions of $CD8^+$ T cells in chronic HIV infection are antigen specific. J. Exp. Med. **188:**785–790.
51. **Yin, L., C. A. Rodriguez, W. Hou, O. Potter, M. J. Caplan, M. M. Goodenow, and J. W. Sleasman.** 2008. Antiretroviral therapy corrects HIV-1-induced expansion of $CD8^+$ $CD45RA^+$ $CD2^-$) CD11a(bright) activated T cells. J. Allergy Clin. Immunol. **122:**166–172.